

# Beam Steering Fabry Perot Array Antenna for mm-Wave Application

Saeid Karamzadeh<sup>1, \*</sup>, Vahid Rafiei<sup>2</sup>, and Mesut Kartal<sup>3</sup>

**Abstract**—Beam-steering antennas especially with Butler matrix feed network are an effective remedy for wireless communications systems troubles such as disruptive effects in mm-wave frequency. In this work, a novel  $4 \times 4$  Butler matrix feed beam steering antenna is designed at 35 GHz. A zeroth order resonance antenna element is used for bandwidth and radiation efficiency increment. To increase the gain of the antenna, a novel mm-wave Fabry Perot layer which is composed of a partially reflective surface is designed. All designing steps are presented.

## 1. INTRODUCTION

Recently, the demands for increasing the speed of data transmission have led to the development of wireless communication applications beyond the K-band. As an undeniable part of mm-wave systems, mm-wave antenna designs have gained importance, and the interest of researchers on this subject has increased gradually. Although many types of antennas have been presented to date, microstrip antennas due to their low profile, low cost, and easy integration have a significant position among researchers. As known, it suffers from limiting the mm-waveband communication range due to its high atmospheric attenuation. To conquer this issue, two general solutions are employed 1) beam steering technique and 2) high gain antenna has been introduced [1–9]. Therefore, in order to design an mm-wave beam steering antenna, it is necessary to have a radiation element which is smaller in size and characteristically stable. On the other hand, in short range systems such as indoor wireless personal area networks (WPAN), it is imperative that the antenna radiates within a wide beamwidth, considering that the user may be in any position [2–4]. Although it is necessary to use a substrate with a high dielectric constant to achieve stable performance in a regular rectangular patch antenna, high dielectric results in narrow bandwidth and low radiation efficiency. In this paper, zeroth order resonance (ZOR) technique is used to solve this problem, as discussed in the following section.

Although the single element problem can be solved by ZOR technique, the problem of mm-wave in terms of beam steering and high gain remains. Principally, a beam steering or beam forming network (BFN) generates amplitudes and phases in accordance with the form of the output pattern to deliver [6, 7]. Even though various methods have been proposed to provide BFNs such as Blass matrix, Nolen matrix, and Rotman lens, the Butler matrix feed network is popular compared to the others due to the theoretically lossless structure and the minimum number of components being hired [6, 7]. Hitherto, a limited number of studies have been concentrated on designing mm-wave microstrip Butler matrix feed networks [8, 9]. In [8], an integrated Butler matrix feed network based on a linear quasi-Yagi array was reported. The maximum antenna gain was about 8.9 dB, and a 3 GHz BW at 60 GHz was covered. In [9], two states of Butler matrix slot antenna were introduced. Each state had the same Butler feed but contained a varied number of slot elements. In the case of a  $2 \times 4$ -slot antenna array, the impedance BWs measured ( $\leq -10$  dB) were at least 0.8 GHz and 0.7 GHz in a similar  $4 \times 4$  array.

---

*Received 1 February 2020, Accepted 27 March 2020, Scheduled 9 April 2020*

\* Corresponding author: Saeid Karamzadeh (karamzadeh@itu.edu.tr).

<sup>1</sup> Electrical and Electronics Engineering Department, Faculty of Engineering and Natural Sciences, Bahçeşehir University, Istanbul, Turkey. <sup>2</sup> Research and Development Department, Microwave and Antenna Group, GraphenePi Company, Istanbul 34400, Turkey.

<sup>3</sup> Department of Electronics and Communication Engineering, Istanbul Technical University, Istanbul, Turkey.

**Table 1.** Performances of the published FP antennas ([i] is the proposed antenna).

Ref	Frq (GHz)	Height of air layer	Number of substrate layers/antenna height	HPBW	Gain
[12]	60	$\lambda_0/2$	$3/0.52\lambda_0$	0.5%	15.2
[13]	94	$\lambda_0/2$	Nonplanar/ $1.02\lambda_0$	1%	13
[14]	35	$\lambda_0/2$	$3/0.67\lambda_0$	7.1%	16.1
[15]	63	$3\lambda_0/10$	$2/0.52\lambda_0$	4.3%	11
[16]	44	no	$1/0.23\lambda_0$	1%	14
[i]	35	no	$3/0.25\lambda_0$	---	----

The maximum gains measured for  $2 \times 4$  and  $4 \times 4$  were approximately 5 and 7 dBi, respectively. As well known, when the beam of the antenna is steered, the antenna gain decreases as a negative aspect of the beam steering antenna. This problem can be overcome by using the reflector technique, but new problems arise, such as increased antenna size and manufacturing problems [10]. Utilizing the Fabry Perot (FP) technique is a proper solution to overcome this problem [11]. In last decade, different mm-wave FP antennas have been stated [9–16]. Table 1 is provided to give a fair comparison among the reported studies [12–15]. As shown in Table 1, the majority of the antennas [12–15] have an air gap between the antenna and the FP layer. Although the use of screws and foam helps to adjust the air gap relatively, the small difference between simulation and fabrication distance in the mm-wave regime can seriously affect the measurement results. To conquer this problem and reduce the antenna size, in some projects the air layers were replaced by dielectric layers [16]. Inspired by [1–3], to address the problem, a broad side pattern antenna element is presented using the ZOR technique. In order to have a band gap between the elements in the frequency range from 33.2 to 36.8 GHz, the antenna elements can be brought closer to each other at a distance of  $0.35\lambda_0$ , as demonstrated below, resulting in an increase in the HPBW of the antenna. To increase the gain of the proposed beam steering antenna, a new mm-wave FP layer consisting of a partially reflective surface (PRS) covering is designed at 35 GHz. The performance of the  $4 \times 4$  elements beam steering FP antenna has a tradeoff among high gain, wide bandwidth, and low profile. Table 1 indicates a comparison between the recent reported FP antennas and the proposed one. The details and results of the proposed antenna are discussed in the following section.

## 2. ANTENNA ELEMENT

The configuration of the proposed single antenna element inspired by [2] is displayed in Fig. 1. It consists of two substrate layers, Rogers 3010 ( $\epsilon_r = 10.2$ ,  $\tan \delta = 0.0035$ ) and RT/Duroid 5880 ( $\epsilon_r = 2.2$ ,  $\tan \delta = 0.0009$ ) with a thickness of 0.25 mm and 0.508 mm, respectively. The feed line substrate layer has a low thickness and high permittivity to prevent unexpected radiation along its path.

The upper substrate layer contains a mushroom structure and a square ring as a resonator which has a common resonance with a slot structure. Indeed, the slot has two substantial roles in the antenna element; the first is to isolate the antenna section and the feed line, and the second is to adjust the resonance frequency of the antenna. The slot provides a directional radiation pattern with TM<sub>010</sub> mode, while the mushroom section with parasitic square ring forms an omnidirectional radiation pattern, the synthesis of the patterns forming a high gain directive pattern with a wide beam width. The optimized values of the antenna dimensions are as follows:  $W_p = 2$  mm,  $W_h = 1.3$  mm, radius of the via ( $V_r$ ) = 0.1 mm,  $L_a = 2$  mm,  $W_a = 0.1$  mm,  $h_1 = 0.508$  mm,  $h_2 = 0.25$  mm,  $L_{\text{stub}} = 1$  mm. The equivalent circuit representing the role of each section of the antenna is shown in Fig. 2 [1, 2]. In this figure,  $C_1, C_a, L_a$  and  $R_a$  illustrate the equivalent circuit model of the aperture resonance circuit, while  $C_p, L_p$  and  $R_p$  are the equivalent circuit of the parasitic ring patch antenna, and  $C_R, L_L$  and  $R_m$  are the equivalent circuit of the mushroom antenna.  $\Gamma_m, \Gamma_p$ , and  $\Gamma_{pm}$  are the coupling coefficients between the aperture and the mushroom, between the aperture and the parasitic ring patch, and between the

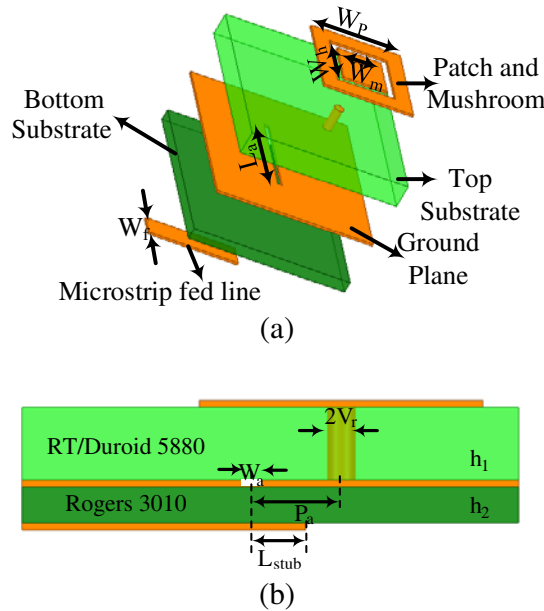


Figure 1. Configuration of proposed ZOR antenna element. (a) Perspective view, and (b) side view.

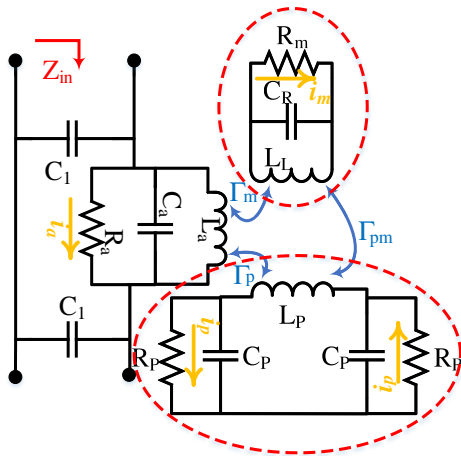


Figure 2. Equivalent circuit of single element.

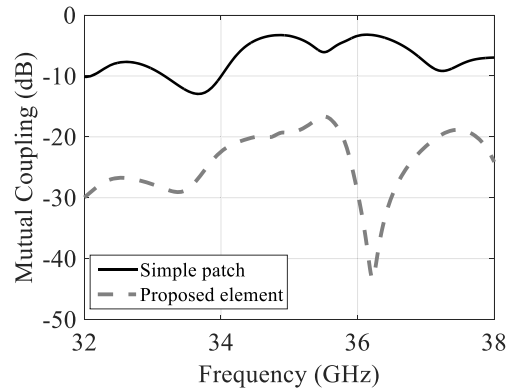
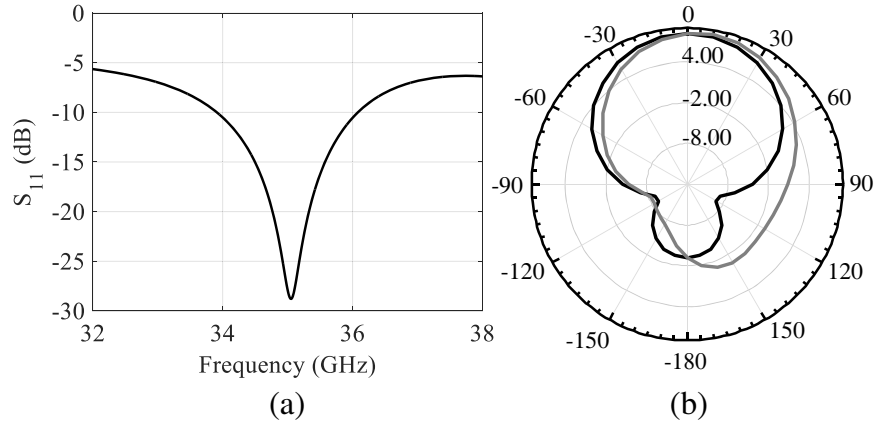


Figure 3. Comparison between simulated mutual coupling of proposed antenna with simple patch in  $0.35\lambda_0$  distance.

mushroom and the parasitic ring patch, respectively. The values obtained for the equivalent circuit are as follows:  $C_1 = 8.82$  fF,  $C_a = 139.54$  fF,  $L_a = 160.99$  nH,  $R_a = 2295 \Omega$ ,  $C_p = 52.61$  pF,  $L_p = 765.08$  nH,  $R_p = 905 \Omega$ ,  $C_R = 92.22$  pF,  $L_L = 206.01$  nH,  $R_m = 778 \Omega$ ,  $\Gamma_m = 0.132$ ,  $\Gamma_p = 0.123$ , and  $\Gamma_{pm} = 0.085$ .

As known, the mushroom structure is generally used as an electromagnetic band gap structure to reduce mutual coupling among antenna elements in the array. Referring to the equivalent circuit structure shown in Fig. 2 and the simulation results for the mutual coupling values given in Fig. 3, it can be clearly seen that two antennas with simple rectangular patches, which are located in a specific distance ( $0.35\lambda_0$ ) from each other instead of proposed mushroom structure, have a higher value (about 13 dB) of mutual coupling. The simulated  $S_{11}$  and radiation pattern of the antenna element are illustrated in Fig. 4. As afore discussed, by adjusting the main resonance with ZOR technique, the proposed antenna results in a single-resonant (Fig. 4(a)), high-gain, and broadside pattern (Fig. 4(b)) response at 35 GHz.



**Figure 4.** The simulated results of proposed antenna elements (a)  $S_{11}$  and (b) radiation pattern at 35 GHz (solid black line is  $\varphi = 0^\circ$  and solid grey line is  $\varphi = 90^\circ$ ).

The proposed antenna has a gain of 7.21 dBi and an  $E$ -plane HPBW of  $138^\circ$ . For more results, please refer to [2].

### 3. PRS CELL DESIGN

As discussed previously, a popular technique in high gain antenna design is the use of Fabry Perot or PRS structures. In this work, as shown in Fig. 5(a), a PRS layer placed on the ZOR antenna is designed, and the structure is excited by the proposed single element. A simple optical ray model can be used to analyze the antenna [8]. The resonant condition of FP antenna can be written by,

$$\varphi_g + \varphi_r - \frac{4\pi h}{\lambda} = 2N\pi \quad N = 0, \pm 1, \pm 2, \dots \quad (1)$$

where  $h$  is the height between the PRS and the ground;  $\varphi_g$  and  $\varphi_r$  are the phase angles of the reflection coefficients of the metal ground plane and the PRS respectively; and  $\lambda$  is the operation wavelength in the substrate [8]. Fig. 5(b) shows that the proposed PRS has a resonance condition at 35 GHz.

Since the ground plane at the bottom of the mushroom and parasitic square ring in this structure is also used as a common ground by the PRS and the antenna element, the effects of the top layer of the antenna element and the common ground in the simulation should be considered.

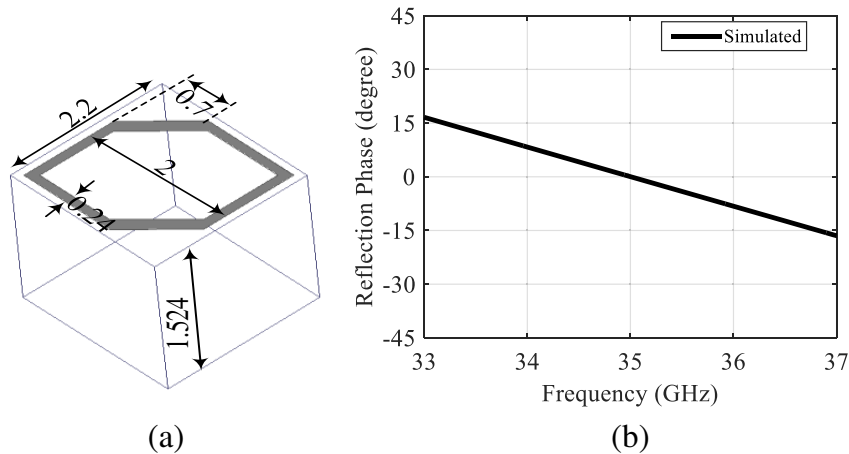


**Figure 5.** (a) Dimensions of the proposed unit cell and (b) reflection coefficient phase angle diagram of PRS unit cell.

#### 4. BUTLER MATRIX AND BROADBAND PHASE SHIFTER

The semi-interdigital broadband phase shifter structure and the phase shift diagram of the proposed structure are shown in Figs. 6(a) and (b), respectively. As can be seen, the phase shifter having a smooth slope indicates that the proposed structure can be used in a broadband application. The configuration of proposed  $4 \times 4$  Butler matrix is displayed in Fig. 7(a). The proposed Butler matrix is based on a 90-degree patch coupler designed to have the advantages of reducing path loss in mm wave, improving insertion loss, and simplicity of fabrication. As discussed, the antenna element having a broadside pattern and single resonance, using a feed network which can provide resonance at ZOR frequency, helps us to attain a high gain antenna with broadside pattern. Therefore, a beam steering Butler matrix feed network having a broadband phase shift and a frequency resonance adopted with the ZOR element is provided. As shown in Figs. 7(b) and (c), a good power division performance between the input and output ports is achieved by providing low loss values, and the magnitude of scattering parameters shows a power divider value of  $-7$  dB at 35 GHz. The proposed Butler matrix is simulated and optimized by the Agilent Advanced Design System (ADS).

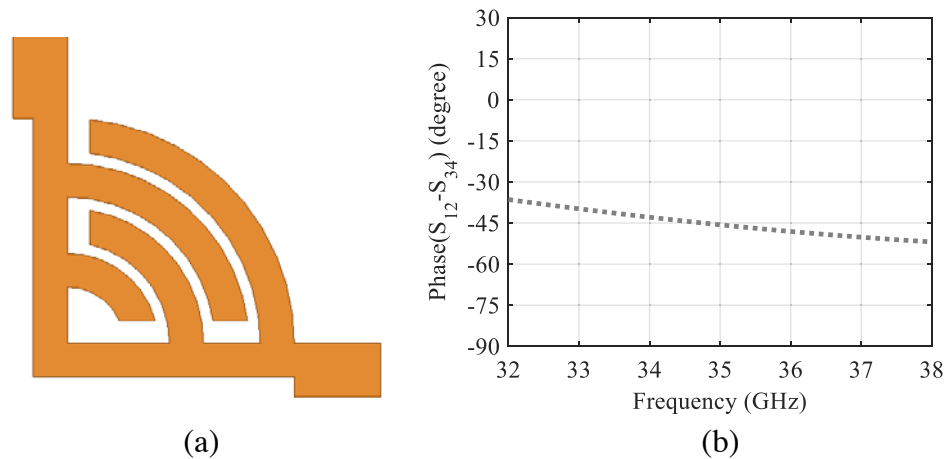
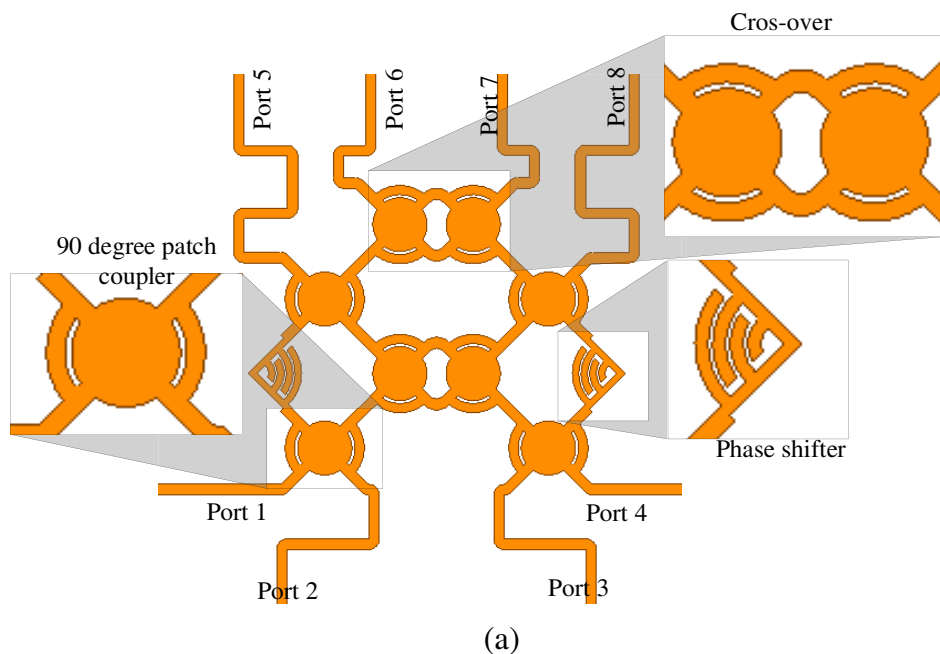
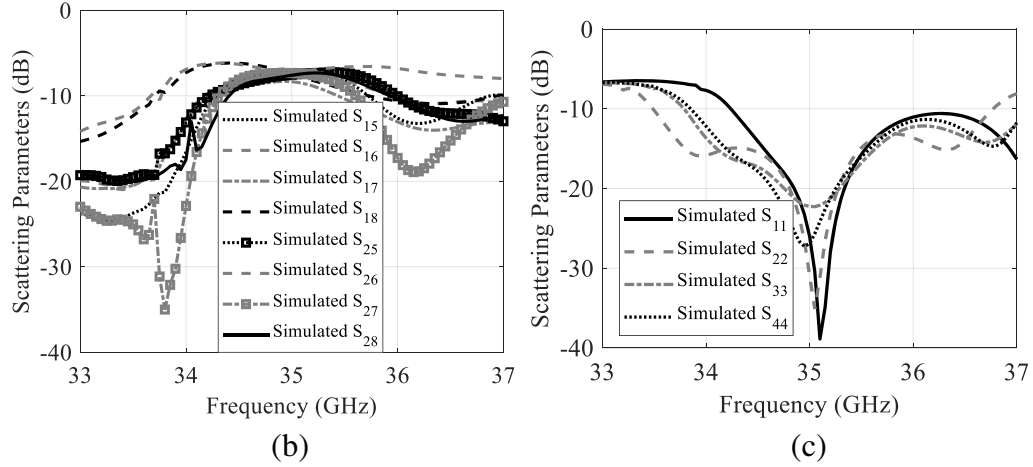


Figure 6. (a) Structure of the broadband  $45^\circ$  phase shifter and (b) resulting phase shift.





**Figure 7.** (a) Configuration of proposed Butler matrix feed network with broadband phase shifter, (b) insertion loss, and (c) reflection coefficients of input ports.

## 5. ANTENNA RESULTS AND DISCUSSION

The hypothesis of a novel 45-degree phase shifter and broadband couplers are induced to a novel low loss  $4 \times 4$  Butler matrix feed network. To overcome short-range effects on mm-wave frequencies, two techniques of broadside single-antenna elements and a feed network with a Butler matrix are presented. The single elements are compact zeroth-order resonance antennas that are fed by the aperture feed technique. Proposed elements to have a structure such as a metamaterial mushroom can be used in a short distance along with low mutual coupling.

The proposed beam-steering array antenna was fabricated and tested to validate the simulated results. Fig. 8 shows the prototype of the fabricated antenna. The scattering parameters of the array antenna were measured by Agilent 8510XF (E7340A) vector network analyzer. Since the Butler matrix is a symmetric structure, only two input ports are measured, and the results can be generalized to the other two ports.

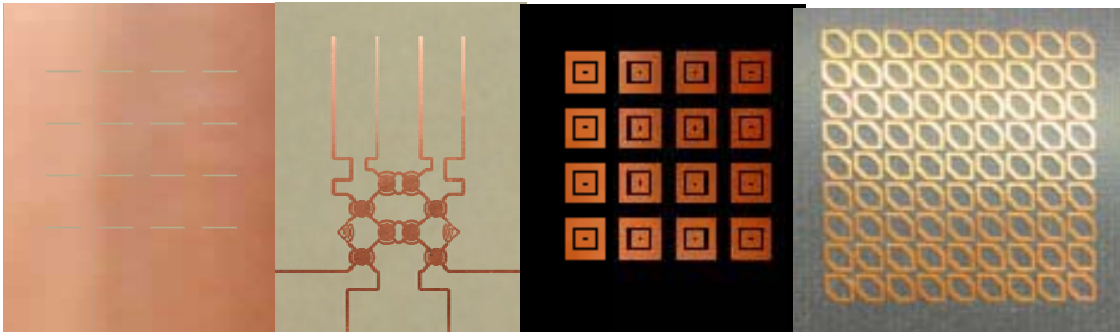


**Figure 8.** Sample prototype of fabricated proposed beam steering antenna.

The similarities between simulated and measured results for  $S_{11}$  and  $S_{22}$  are displayed in Fig. 9. There is a good match between the simulated and measured results across the entire frequency band with a small frequency shift. The measured results cover a frequency range from 32.11 to 37.86 GHz.

The 3D simulated radiation patterns of the antenna at 35 GHz for ports 1, 2, 3, and 4 are shown in Fig. 10. The normalized measured radiation patterns of the planar microstrip  $4 \times 4$  antenna array at 35 and 37 GHz with the proposed Butler matrix are displayed in Fig. 11. As can be clearly seen in

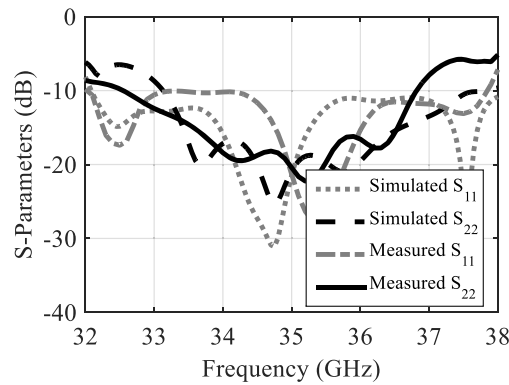


Figure 9. Comparison between simulated and measured results for  $S_{11}$  and  $S_{22}$ .

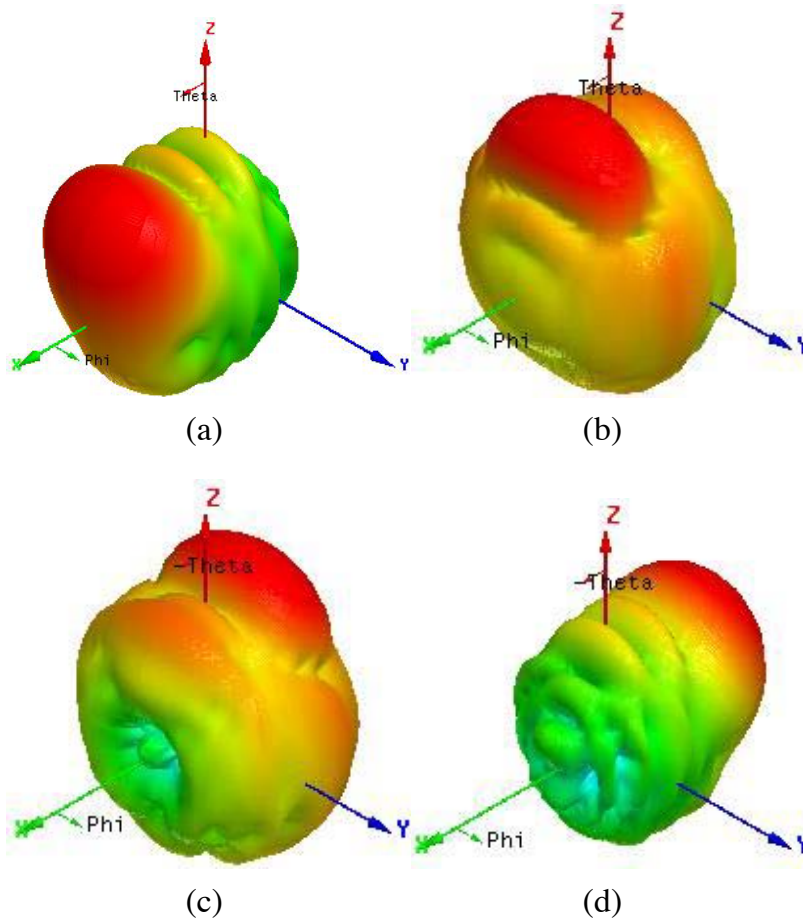
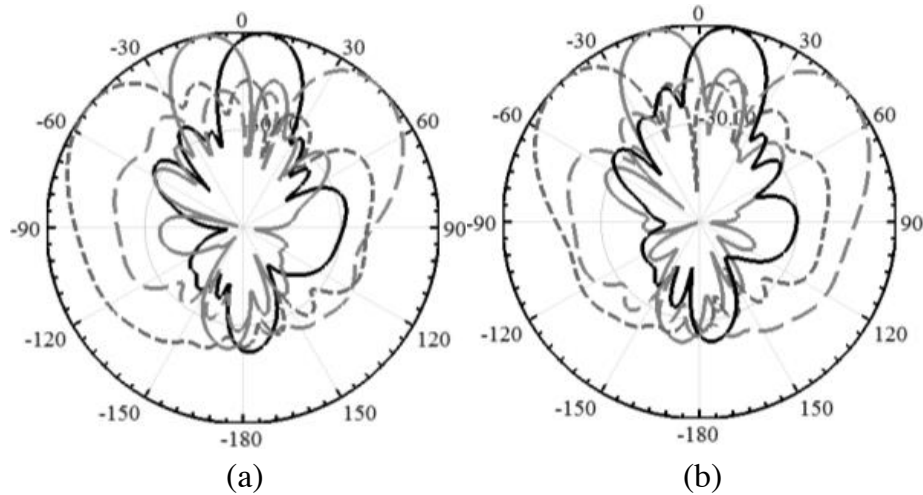


Figure 10. Simulated 3D radiation patterns corresponding to ports 1–4 at 35 GHz: (a) port 1, (b) port 2, (c) port 3, and (d) port 4.

the figure, the pattern direction is changed by changing the input ports. The beams were successfully steered with peak gains ranging from 17.8 to 18.9 dBi for ports 1 and 2, respectively. With this novel design comprising 16 ( $4 \times 4$ ) mentioned elements with  $0.35\lambda$  in between and FP layer a broadband and high-gain beam steering array antenna for maximum input of impedance bandwidth of 32–38 GHz and a scan angle of about  $\sim 93^\circ$  was attained. The aim of designing proposed antenna is an implementation of a novel beam steering antenna with high gain and broadside pattern.



**Figure 11.** Normalized measured radiation patterns of the planar microstrip antenna array at (a) 35 and (b) 37 GHz for port 1 as dashed line, port 2 as solid line.

## 6. CONCLUSION

In this work, a new high gain beam steering antenna has been introduced. Taking advantage of the novel design, a compact and broadband beam steering array antenna with the ability of covering impedance bandwidths (from 32.11 to 37.86 GHz) and scanning a solid angle of about  $\sim 93^\circ$ , with a peak gain of 18.9 dBi, has been achieved. The proposed beam-steering array antenna was fabricated and measured. There is a good agreement between the simulated and measured results across the entire frequency band. The proposed antenna could be used in many mm-wave applications such as automotive radar and the 5G mobile applications.

## REFERENCES

1. Ko, S. T. and J. H. Lee, "Aperture coupled metamaterial patch antenna with broad  $E$ -plane beamwidth for millimeter wave application," *2013 IEEE Antennas and Propagation Society International Symposium (APSURSI)*, 1796–1797, Orlando, FL, 2013, doi: 10.1109/APS.2013.6711557.
2. Lee, C.-H. and J.-H. Lee, "Millimeter-wave wide beamwidth aperture-coupled antenna designed by mode synthesis," *Microw. Opt. Technol. Lett.*, Vol. 57, 1255–1259, 2015, doi: 10.1002/mop.29058.
3. Ko, S. T. and J. H. Lee, "Hybrid zeroth-order resonance patch antenna with broad  $E$ -plane beamwidth," *IEEE Transactions on Antennas and Propagation*, Vol. 61, No. 1, 19–25, Jan. 2013, doi: 10.1109/TAP.2012.2220315.
4. Artemenko, A., A. Mozharovskiy, A. Maltsev, R. Maslennikov, A. Sevastyanov, and V. Ssorin, "Experimental characterization of E-band two-dimensional electronically beam-steerable integrated lens antennas," *IEEE Antennas and Wireless Propagation Letters*, Vol. 12, 1188–1191, 2013, doi: 10.1109/LAWP.2013.2282212.
5. Gheethan, A., M. C. Jo, R. Guldiken, and G. Mumcu, "Microfluidic based Ka-band beam-scanning focal plane array," *IEEE Antennas and Wireless Propagation Letters*, Vol. 12, 1638–1641, 2013, doi: 10.1109/LAWP.2013.2294153.
6. Karamzadeh, S., V. Rafii, M. Kartal, and B. S. Virdee, "Compact and broadband  $4 \times 4$  SIW Butler matrix with phase and magnitude error reduction," *IEEE Microwave and Wireless Components Letters*, Vol. 25, No. 12, 772–774, Dec. 2015, doi: 10.1109/LMWC.2015.2496785.
7. Karamzadeh, S., V. Rafii, M. Kartal, and B. S. Virdee, "Modified circularly polarised beam steering array antenna by utilised broadband coupler and  $4 \times 4$  Butler matrix," *IET Microwaves, Antennas & Propagation*, Vol. 9, No. 9, 975–981, Jun. 18, 2015, doi: 10.1049/iet-map.2014.0768.

8. Haraz, O. M. and A. R. Sebak, "Two-layer butterfly-shaped microstrip  $4 \times 4$  Butler matrix for ultra-wideband beam-forming applications," *2013 IEEE International Conference on Ultra-Wideband (ICUWB)*, 1–6, Sydney, NSW, 2013, doi: 10.1109/ICUWB.2013.6663812.
9. Alreshaid, A. T., M. S. Sharawi, S. Podilchak, and K. Sarabandi, "Compact millimeter-wave switched-beam antenna arrays for short range communications," *Microw. Opt. Technol. Lett.*, Vol. 58, 1917–1921, 2016, doi:10.1002/mop.29940.
10. Hu, W., M. Arrebola, R. Cahill, et al., "94 GHz dual-reflector antenna with reflectarray subreflector," *IEEE Transactions on Antennas and Propagation*, Vol. 57, No. 10, 3043–3050, 2009.
11. Von Trentini, G., "Partially reflecting sheet arrays," *IRE Transactions on Antennas and Propagation*, Vol. 4, No. 4, 666–671, 1956.
12. Sauleau, R., P. Coquet, and T. Matsui, "Low-profile directive quasi-planar antennas based on millimetre wave Fabry-Perot cavities," *IEE Proceedings — Microwaves, Antennas and Propagation*, Vol. 150, No. 4, 274–278, 2003.
13. Lee, Y., X. Lu, Y. Hao, S. Yang, J. R. G. Evans, and C. G. Parini, "Low-profile directive millimeter-wave antennas using free-formed three-dimensional (3-D) electromagnetic bandgap structures," *IEEE Transactions on Antennas and Propagation*, Vol. 57, No. 10, 2893–2903, 2009.
14. Tan, G.-N., X. Yang, H.-G. Xue, and Z. Lu, "A dual-polarized Fabry-Perot cavity antenna at Ka band with broadband and high gain," *Progress In Electromagnetics Research C*, Vol. 60, 179–186, 2015.
15. Hosseini, A., F. Capolino, and F. De Flaviis, "Gain enhancement of a V-band antenna using a Fabry-Perot cavity with a self-sustained all-metal cap with FSS," *IEEE Transactions on Antennas and Propagation*, Vol. 63, No. 3, 909–921, 2015.
16. Hosseini, S. A., F. Capolino, and F. De Flaviis, "Q-band single layer planar Fabry-Perot cavity antenna with single integrated-feed," *Progress In Electromagnetics Research C*, Vol. 52, 135–144, 2014.